



CHEMICAL FOOTPRINT OF THE SOLVENT SOLUBLE EXTRATERRESTRIAL ORGANIC MATTER OCCLUDED IN SOŁTMANY ORDINARY CHONDRITE

Philippe SCHMITT-KOPPLIN^{1,2}, Mourad HARIR¹, Basem KANAWATTI¹,
Dimitrios TZIOZIS¹, Norbert HERTKORN¹, Zelimir GABELICA³

¹ Helmholtz-Zentrum Muenchen, German Research Center for Environmental Health,
Analytical BioGeoChemistry, Ingolstaedter Landstrasse 1, D-85764 Neuherberg, Germany

² Chair of Analytical Food Chemistry, Technische Universität München, D-85354 Freising-Weißenstephan, Germany

³ Université de Haute Alsace, ENSCMu, Lab. GSEC, 3, Rue A. Werner, F-68093 Mulhouse Cedex, France

Abstract: By characterizing organic molecules of extra-terrestrial origin included in the Sołtmany meteorite, we also present the first results of the non-targeted chemical analysis of the methanol soluble organic matter present in an L6 ordinary chondrite. The structural characterization by means of ultrahigh resolution Fourier transform ion cyclotron mass spectrometry (FT-ICR-MS) with electrospray ionization (ESI) in negative and positive modes demonstrated an unexpected and astonishing chemical diversity with several thousand mass peaks that could be converted into C, H, N, O, S, and P elemental compositions. Molecular signatures were typically those of considerably oxygenated CHO and CHOS molecular series of primarily aliphatic character. ¹H nuclear magnetic resonance (NMR) spectroscopy confirmed the prevalent existence of pure and functionalized aliphatic spin systems of intermediate chain length (C₃₋₄ units), oxygenated aliphatics and a considerable diversity of oxygenated aromatics in the proton-based abundance ratio near 24 : 2 : 1. Although only residual organic matter allegedly survives in highly thermally altered L6 chondrites, the physical protection of organic matter in microcavities and traps between mineral surfaces might have supported and governed the chemistry with an apparent recalcitrance of extraterrestrial organic matter (EOM). Future studies of the organic matter in ordinary chondrites and its composition and structure in various regimes of (e.g.) temperature, radiation, pressure, and water content could shed light on these meteorites' formation and evolution.

Keywords: ordinary chondrite, extraterrestrial organic matter, carbon, nitrogen, sulphur, meteorite, Sołtmany, nuclear magnetic resonance spectroscopy (NMR), Fourier transform ion cyclotron resonance mass spectrometry (FT-ICR-MS)

INTRODUCTION

Chondrites comprise the most common types of meteorites and are expected to represent the most primitive ones as well. Chondrites have been processed to various degrees through thermal metamorphism, water alteration, and/or shock metamorphism. Their classification is mainly based upon their elemental and stable isotope compositions as well as their petrological characteristics, which enable one to reconstitute their history in accordance with the minerals present (Weis-

berg et al., 2006). Only limited information is available in the literature on the organic matter and carbon content speciation in ordinary chondrites. This carbon is mainly separated into three components: (i) soluble organic matter (SOM), (ii) insoluble organic matter (IOM) and (iii) graphite, either in metal grains or in the matrix. These carbon phases (easily recovered from primitive type 3 OCs like Semarkona) have been processed via intense thermal metamorphism in type

Corresponding author: Philippe SCHMITT-KOPPLIN, schmitt-kopplin@helmholtz-muenchen.de

6 chondrites. Several techniques are commonly used for examining the metamorphic gradation of organic matter in unequilibrated ordinary chondrites. Raman spectroscopy is one of these methods (Quirino et al., 2003), as are infrared spectroscopy (Kebukawa et al., 2011) and XANES at the carbon edge (Cody et al., 2008). However, Raman spectroscopy has reached its limits in higher petrologic types (5, 6), in which graphite is established as the main persisting form of carbon. The analysis of organic compounds has often been directed towards trace classes of organic compounds such as polyaromatic hydrocarbons and amino acid derivatives (Zenobi et al., 1992; Herd et al., 2011). These petrologic studies attempt to understand the early history of our solar system from the record preserved in meteorites (Alexander et al., 2001). It is well known that both water and carbon contents decrease with increasing petrologic type (Fig. 1). Studies

on solvent extractions of ordinary chondrites are rarely found in literature, and the few results illustrated in Fig. 1 show that the carbon content for L6 type meteorites analysed thus far is close to 0.25%. Softmany is classified as an L6, W0, S2 type chondrite, which has experienced thorough thermal alteration (Karwowski et al., 2011; Karwowski, 2012). Measurable amounts of carbon were expected to remain within the meteorite, mainly as graphite.

The aim of this contribution was to present our preliminary results on the characterization of the methanol soluble organic fraction present in the Softmany L6 meteorite. Here, high-resolution organic structural spectroscopy, composed of Fourier transform ion cyclotron mass spectrometry (FT-ICR-MS) and NMR spectroscopy, revealed an astonishingly large chemical diversity of EOM with many thousands of distinct CHNOS elemental compositions.

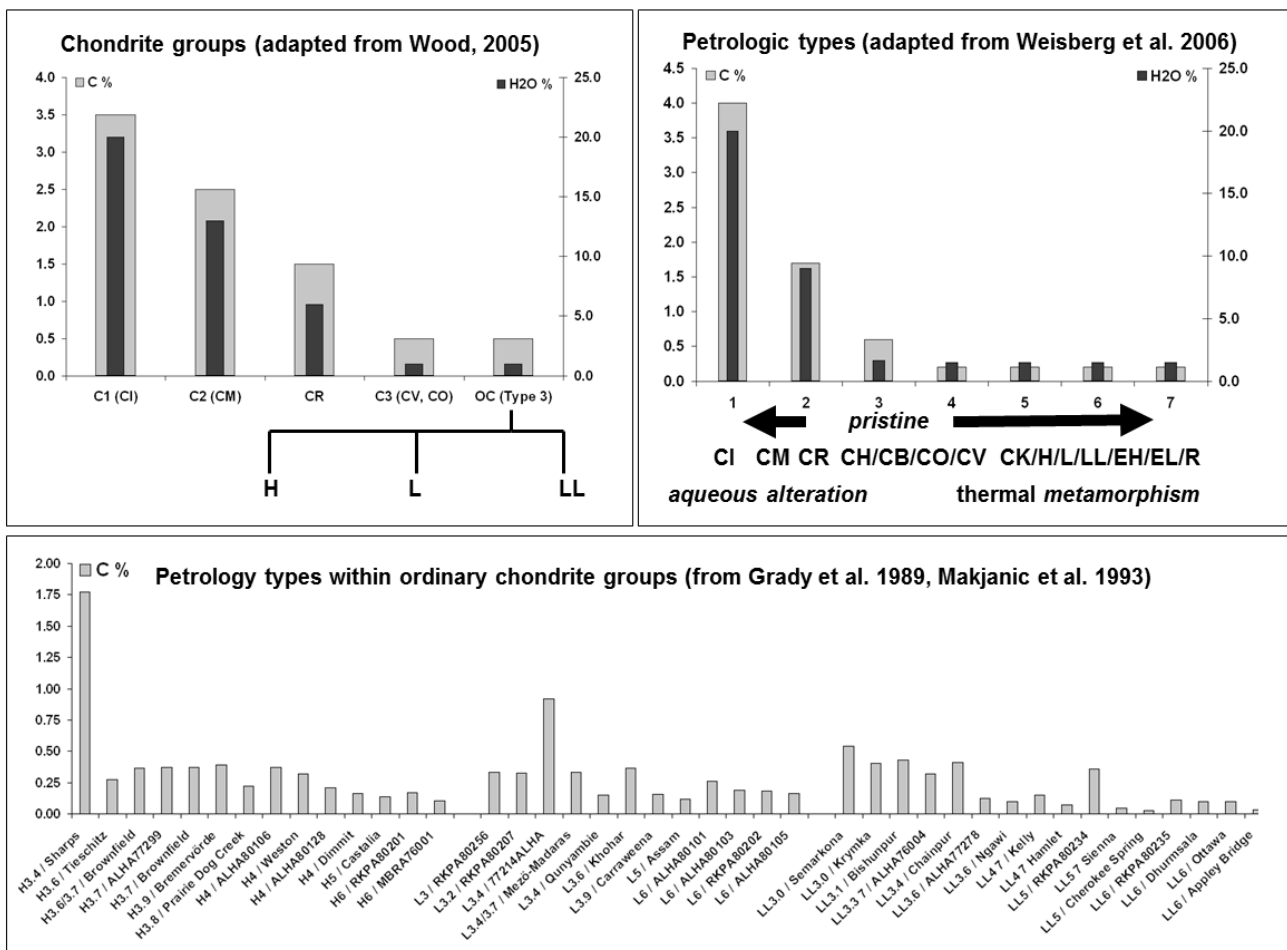


Fig. 1. Carbon and water contents as a function of the petrologic groups and types of meteorites. As an L6 type chondrite, Softmany is expected to show low concentrations of total carbon in the same range as L6 ordinary chondrites conserved in Antarctica

EXPERIMENTAL SECTION

The Sołtmany ordinary chondrite fell on April 30, 2011 at 6:03 CEST through a roof and onto a concrete step in a farm in the village of Sołtmany, Poland, 54°00.53'N, 22°00.30'E (Fig. 2). On May 2, fragments of the stone were purchased and distributed among laboratories for examination. It was classified as an equilibrated ordinary chondrite (L6), W0, S2 (Karwowski et al. 2011; Karwowski, 2012) and some articles describe its mineralogy and petrography in more detail in this special issue on the Sołtmany fall.

A fragment was obtained for analysis from Tomasz Jakubowski and Prof. Tadeusz A. Przylibski, Wrocław University of Technology, Institute of Mining Engineering, Wrocław, Poland.

Sample preparation

Extracts for FT-ICR-MS analysis were prepared as described previously in Schmitt-Kopplin et al. (2010). An intact piece of dry meteorite weighing about 50 mg was briefly washed with methanol (rapid contact with 1 mL methanol that was subsequently discarded), immediately crushed in an agate mortar with 1 mL of LC/MS grade methanol, and transferred into an Eppendorf tube within an ultrasonic bath for 3 minutes. The tube was then centrifuged for 5 min. The supernatant methanol extract was directly used for FT-ICR-MS infusion. NMR samples were prepared similarly, but using CD₃OD as the solvent (cf. NMR experimental section). Prior to the sample extraction, great care was used to clean the agate pillar with an ultrasonic bath and solvent. A blank sample was produced by following the same extraction procedure without a meteorite fragment, and this was analysed before and after each meteorite analysis. No significant peaks in the mass range of the meteorite extracts were observed; a detail of a blank mass spectrum is shown in Fig. 4.

Fourier transform ion cyclotron resonance mass spectrometry (FT-ICR-MS)

In order to fully exploit the advantages of FT-ICR-MS and maintain accuracy, we routinely perform internal calibration on arginine clusters prior to any analysis. Relative m/z errors were usually < 100 ppb across a range of $150 < m/z < 1,500$. The average mass resolution ranged near 400,000 at nominal mass 400. It is noteworthy for readers not familiar with advanced mass spectrometry to understand that this exceptional mass accuracy and mass resolution allows us to assign the exact mass of molecular ions and their respective elemental compositions from mixtures – with better precision than the mass of an electron (which

amounts to $9.10938215 \times 10^{-31}$ kg or 1/1836.2 of the mass of a proton). Accordingly, two molecular compositions with mass differences smaller than that of a single electron mass can be differentiated. Mass peak amplitudes grow with the square root of the number of acquired transients, similarly to NMR spectroscopy (see insert principles of FT-ICR-MS). Sołtmany methanol extracts spectra in our study were measured in negative and positive electrospray ionisation modes [ESI(-) and ESI(+)] under conditions described above (Schmitt-Kopplin et al., 2010); 2,000 scans were accumulated with a total of 4 million data points. The conversion of the exact masses into elementary compositions is shown in more detail in Tziotis et al., 2011. The representation of complex FT-ICR-MS datasets is explained in detail in a book chapter on environmental mass spectrometry (Schmitt-Kopplin et al., 2012); an in-depth analysis of complex secondary organic aerosol extracts and especially a van Krevelen diagram with model compounds indicated can be found in Schmitt-Kopplin et al. 2010.

Nuclear magnetic resonance spectroscopy (NMR)

Proton NMR spectra of methanolic meteorite extracts were acquired with a Bruker Avance NMR spectrom-



Fig. 2. The Sołtmany “hammer” fall. Photos with courtesy from T. Jakubowski

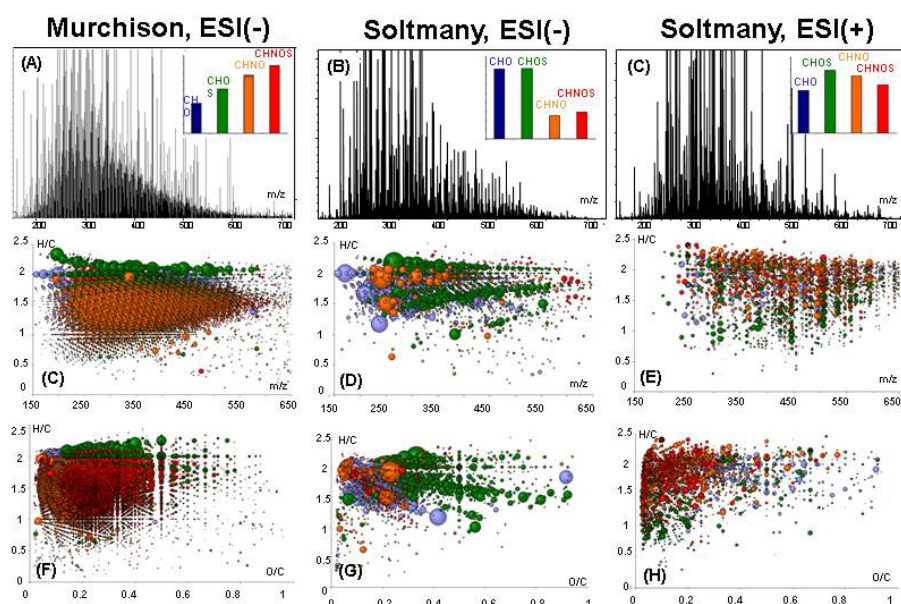


Fig. 3. FT-ICR mass spectra of methanolic extract of Murchison CM2 in ESI(-), Soltmany L6 in ESI(-) and ESI(+) (from left to right) ionization mode, showing (panels A-C) mass peaks in the range of 150 to 700 Daltons – a detailed region of nominal mass 319 of Murchison and Soltmany in ESI(-) ionization mode is shown in Fig. 4, respectively. The corresponding inserted histograms show the relative abundances of the CHO, CHOS, CHNO, and CHNOS ions. (Panels C-E): mass resolved H/C diagram showing the chemical series of compounds according to m/z ; (panels F-H) H/C versus O/C van Krevelen diagrams (Schmitt-Kopplin et al., 2010), revealing (panel D) the rather aliphatic oxygenated character of the Soltmany methanol extractable organic compounds compared to Murchison in ESI(-) mass spectra, whereas (panel H) van Krevelen diagrams of ESI(+) mass spectra revealed the relatively nitrogen- and sulphur-rich and low-oxygenated character of the Soltmany methanol extractable organic compounds (in orange and green colour respectively). In panel D through H diagrams, bubble size is related to the m/z intensity in corresponding mass spectra. The colour code indicates the respective CHO, CHNO, CHOS, and CHNOS molecules

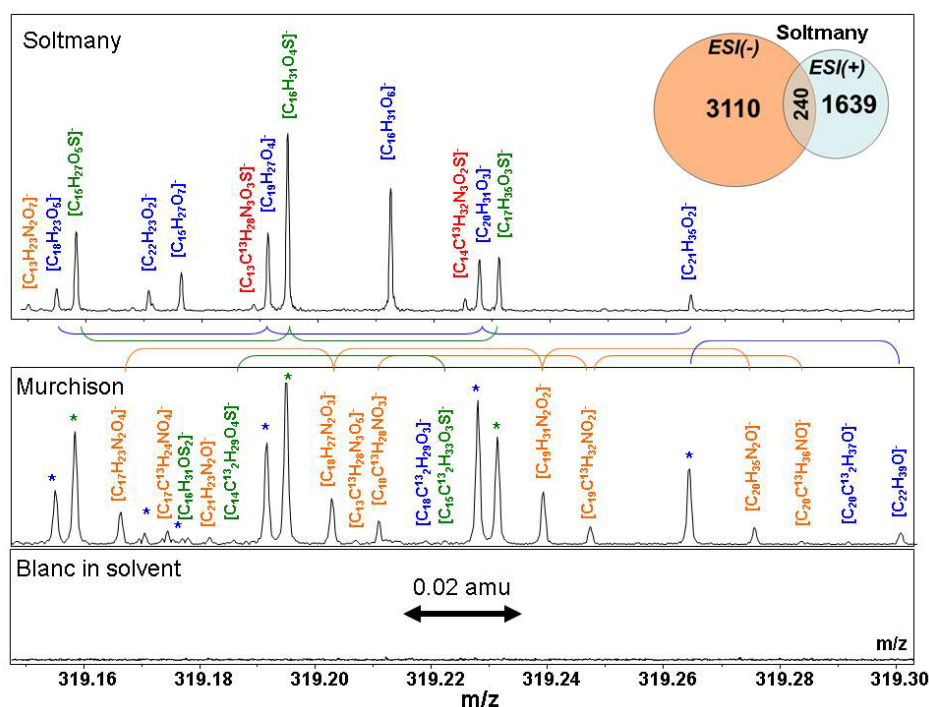


Fig. 4. Detail of a 150 millimass region in the nominal mass 319 of Soltmany L6 negative electrospray FT-ICR mass spectrum compared to the Murchison CM2 presented in our previous study (Schmitt-Kopplin et al., 2010) and the blank methanol extract without meteorite, showing the different signals with their annotations in elementary compositions in CHNOS and ^{13}C -bearing isotopologues. Common elemental compositions in Soltmany and Murchison chondrites are denoted with an asterisk “*”. Also presented is the Venn diagram showing the presence of only a few common elementary formulas in both ESI(-) and ESI(+) mass spectra of the Soltmany extract. Most of the formulas found with electrospray ionization are specific to the negative or positive ionization mode indicating considerable ionization selectivity in electrospray FTICR mass spectra.

eter at 800.35 MHz ($B_0 = 18.8$ T) and 283 K from a few mg of solid (extensively washed with CD_3OD) crushed under 3 mL CD_3OD (Merck, 99.95% 2H). 1H NMR spectra were acquired following evaporation from approx. 70 μL CD_3OD (Merck, 99.95% 2H) solution with a 5 mm z-gradient $^1H / ^{13}C / ^{15}N / ^{31}P$ QCI cryogenic probe in a sealed 2 mm Bruker MATCH tube. 1D 1H NMR spectra were recorded with standard pre-saturation (noesypr1d) to attenuate present residual water (90° excitation pulses 1H : 10 μs , 5 s acquisition time, 5 s relaxation delay, 1 ms mixing time, 4385 scans, 1 Hz exponential line broadening).

A phase-sensitive, gradient-enhanced TOCSY NMR spectrum (mixing time 70 ms) with solvent suppression (dipsi2etpgpsi19) was acquired with an acquisition time of 1 s, a relaxation delay of 2 s, a spectral width of 9615 Hz (12 ppm), via echo-antiecho selection and sensitivity enhancement. 12 scans and 572 increments were acquired and computed to a $16k \times 1024$ matrix with 2.5 Hz exponential multiplication in F2 and a $\pi/4$ shifted sine bell in F1. The NMR spectra of C_3H_8O (Fig. C; app. 2) were computed with Advanced Chemistry Development (ACD, Toronto, Canada) software, H NMR predictor, 2012 release.

RESULTS AND DISCUSSION

The analysis of the methanol extracts resulted in ~14,000 resolved mass peaks in ESI(-) mass spectra (Fig. 3B) and ~7,100 resolved mass peaks in ESI(+) mass spectra (Fig. 3C). In ESI(-) these were converted into initially ~4,100 elemental compositions of which ~3,300 could be confirmed considering the elements C, H, N, O, and S based on the NetCalc compositional approach presented in Tziotis et al., 2011. All of these compositions can be represented via van Krevelen diagrams showing the atomic ratios H/C versus O/C in a colour code for the CHO, CHNO, CHOS and CHNOS type of molecules and a dot size related to the intensity of the related peaks in the mass spectra; the isotopologues are not shown in this representation to avoid structural information redundancy. Soltmany methanolic extract showed a much lower number of mass peaks (and assigned elemental compositions) than did Murchison CM2 methanolic extract (described in detail recently in Schmitt-Kopplin et al., 2010), as illustrated in Fig. 3A. Great emphasis was placed on the cleanliness of working conditions, including comparison with blank samples (same extraction and analysis procedure without meteorite sample). These blanks were almost devoid of mass peaks, clearly demonstrating that the observed mass peaks were solely generated from the meteorite and not from (solvent and/or other) contaminations.

The classification of the elemental composition according to CHO, CHOS, CHNO and CHNOS molecular series showed the importance of highly oxygenated aliphatic sulphur containing compounds in ESI(-) mass spectra (green dots in Fig. 3) whereas, in ESI(+) mass spectra, sulphur compounds were found to exhibit higher aromaticity (lower H/C domain), probably of heterocyclic origin (Fig. 3H). In ESI(-) mass spectra, the CHOS compounds were equally abundant as the CHO compounds, with lesser con-

tributions of CHNOS and CHNO molecules (Fig. 3C and 3D), whereas in ESI(+) mass spectra, many nitrogen containing compounds were nicely ionized as well. These CHNO molecules with low oxygen contents were found across the entire m/z range up to higher molecular masses (Fig. 3D-F).

Further detail of the ESI(-) mass spectrum is shown in Fig. 4 and directly compares to the well-described chemical diversity of the CM2 carbonaceous chondrite Murchison, presented recently in Schmitt-Kopplin et al., 2010. Some elemental compositions were found simultaneously in both Soltmany and Murchison (CHO and CHOS molecular series), across all nominal masses. Coarsely, the structural specificity corresponded to high amounts of nitrogen compounds (CHNO molecules) in Murchison and to large amounts of oxygenated hydrocarbons (CHO molecules) in the Soltmany meteorite. Electrospray ionization primarily ionizes polar compounds with concomitant selectivity in the type of molecules we can "see" with this analytical tool (Hertkorn et al., 2008); additional methods of ionization involving photo- and laser-ionization, which also ionize hydrocarbons, are currently being developed and implemented. FT-ICR mass spectrometry provides unsurpassed resolution and assessment of chemical diversity; it allows for the differentiation of most elemental compositions with the elements C, H, N, O, and S up to a mass of around m/z 600 (Kim et al., 2006). However, this method commonly cannot discriminate between isomers (Hertkorn et al., 2007). It is important to note that the structural disparity of molecular ions grows with decreasing mass difference; i.e. more closely-spaced pairs of mass peaks exhibit ever-increasing mandatory compositional and structural dissimilarity (Hertkorn et al., 2008).

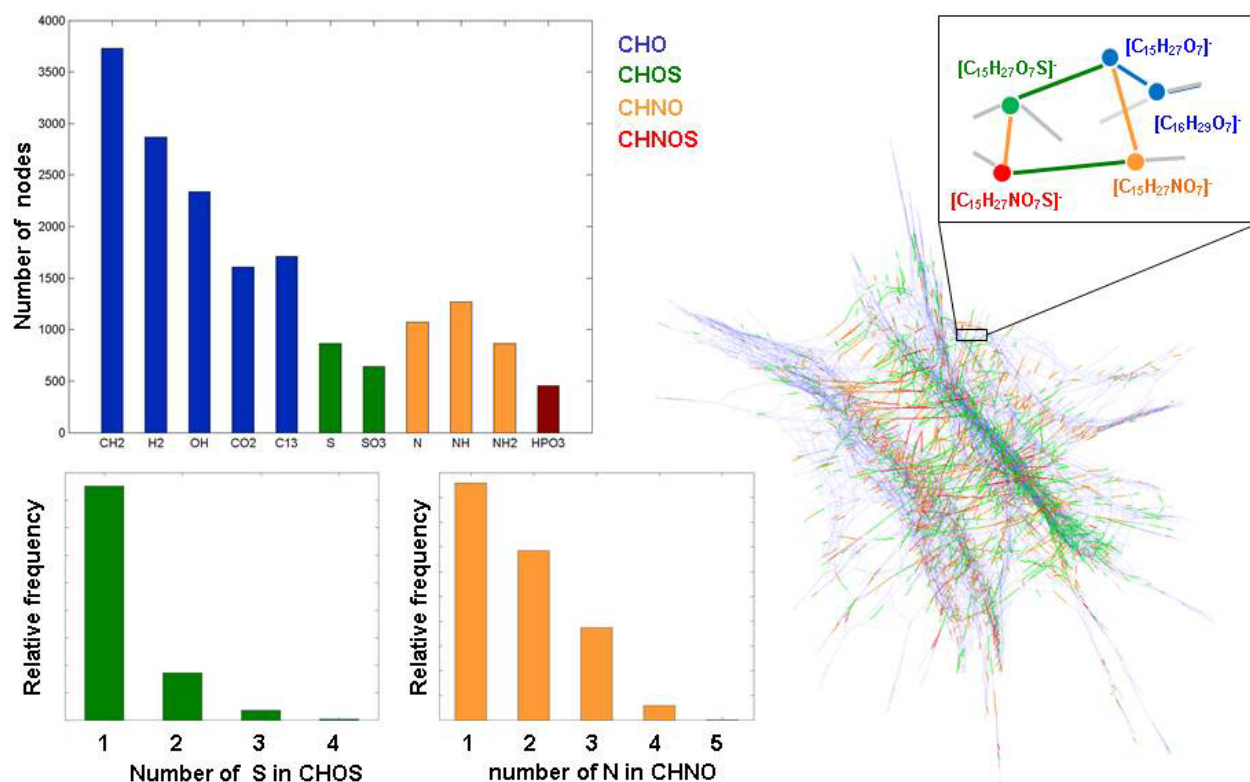


Fig. 5. Relative frequency distribution in the mass differences of Soltmany methanolic extract as obtained with the functional network approach from ESI(-) FT-ICR mass spectra (Tziotis et al., 2010) indicating the count of the exact mass differences corresponding to the different functional groups ($-\text{CH}_2$, $-\text{H}_2$, $-\text{OH}$, $-\text{CO}_2$...). Also shown is the relative abundance of formulas bearing one to four sulphur atoms (S in CHOS_{1-4} molecules) or nitrogen atoms (N in CHN_{1-5}O molecules). The right panel shows the obtained 3D-network of the mass spectral data with a corresponding colour code. The clustering of colors and the different quality of arrangements within CHO (butterfly), CHOS (disk shape with scatter), CHNO (diffuse cloud) and CHNOS (aligned scatter) molecular series indicates structural preferences of sulphur- and nitrogen-containing chemical environments. The insert indicates some connectivities of the molecular ion $\text{C}_{15}\text{H}_{27}\text{O}^-$ provided in Fig. 4.

The elemental compositions were computed using a self-developed software presented previously (Tziotis et al., 2011), which enabled us to generate a compositional space based on the exact experimental mass data with better coverage than has been attained in classical analyses. This algorithm computes differences between two precise experimental masses corresponding to the various atoms (compositional approach) or functional groups (functional approach). The frequencies of these selected mass differences can be represented in diagrams such as those shown in Fig. 5. As is typical for mixtures of organic molecules, the main nominal transformations counted in the Soltmany meteorite were methylene, CH_2 ($\Delta m = \pm 14.0024$ Da), followed by H_2 (double bond equivalent, DBE, $\Delta m = \pm 2.1057$ Da). The structures present in the Soltmany meteorite were highly hydroxylated (OH) and carboxylated (CO_2). Counting the number of sulphurs and nitrogens in all of the obtained elemental compositions showed that most of the CHOS/CHNOS molecules each contain only one sulphur. Nitrogen was found up to three times in CHNO/CHNOS compositions.

Finally, the experimental data can be visualized in a coloured network showing a rather loose structure (Fig. 5).

Non-target organic structural spectroscopy of Soltmany L6 chondrite methanolic extract, in which we attempted to unselectively characterize the soluble polar carbon present, has revealed the considerable chemical diversity of extraterrestrial organic matter (EOM). The short temporal lag period between the stone's fall, sampling, and data acquisition suggests the dominance of EOM with very limited, if any, terrestrial impurities present. FT-ICR mass spectrometry of EOM detects gas-phase molecular ions and allows for an unprecedented resolution of several thousands of molecular formulae directly out of the mixture, and the recognition of very minute quantities of individual molecular compositions. The use of electrospray ionization in FT-ICR mass spectrometry emphasized the detection of polar compounds and discriminated against hydrocarbons and other functionalized organic molecules with nearly absent exchangeable protons (Hertkorn et al., 2008). Hence, the already appreci-

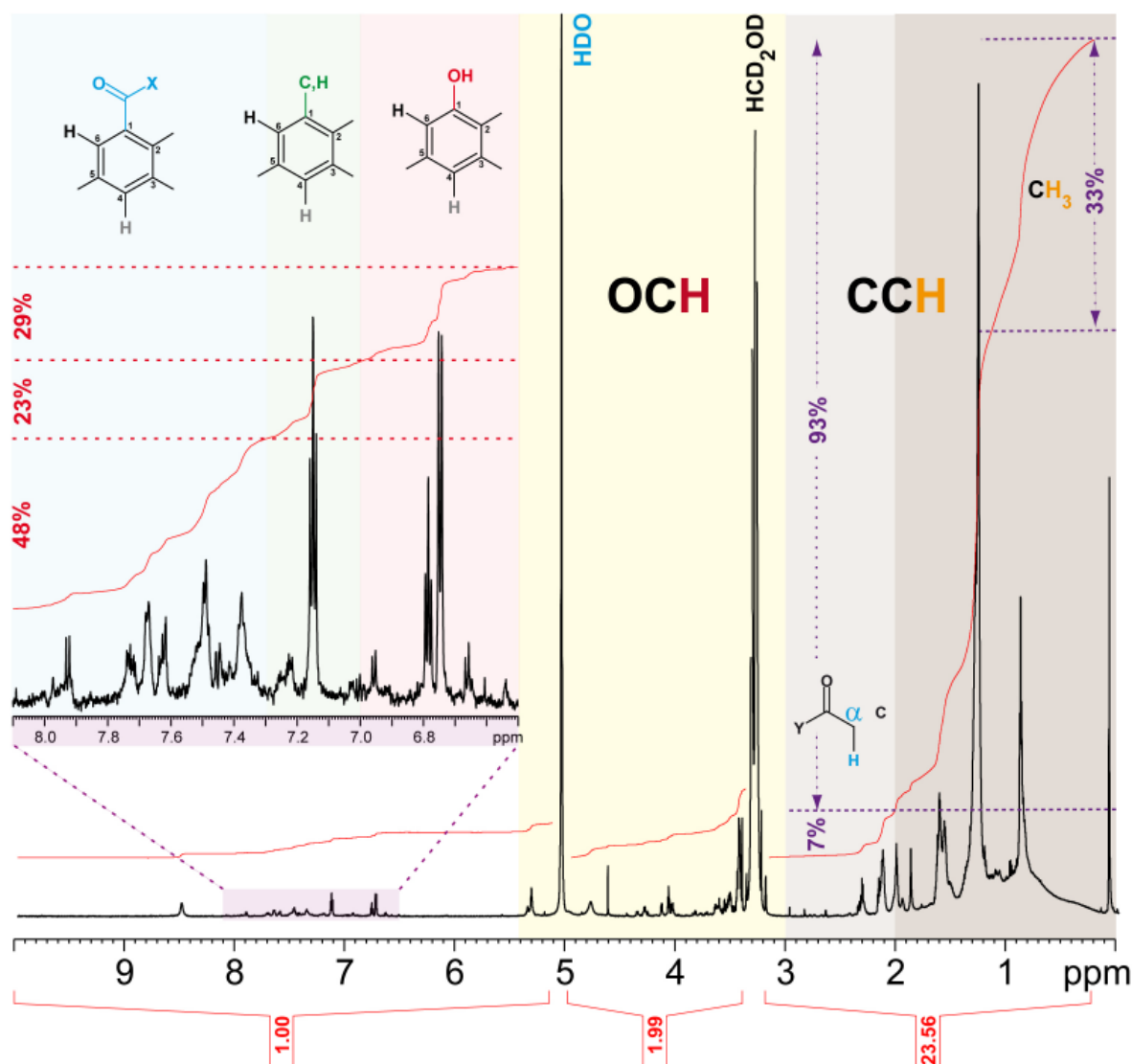


Fig. 6. 800 MHz ^1H NMR spectrum of methanolic extract of Soltmany meteorite with fundamental substructures indicated (cf. text) and expansion of aromatic NMR resonances shown ($\delta_{\text{H}} \sim 6.5 \dots 8.1$ ppm, cf. Figure 7, panel C). Unbroken trails denote proton NMR integrals of main substructure regimes [abundance ratio of unsaturated and doubly oxygenated $\text{C}\underline{\text{H}}$ (O_2CH) : singly oxygenated (OCH) : carbon-bound (CCH) ranged near 1 : 2 : 24]. Aliphatic carbonyl derivatives (i.e. probably carboxylic acids) accounted for nearly 7% of CCH proton NMR section integral ($\delta_{\text{H}} \sim 2.0 \dots 3.1$ ppm; see Fig. 7). Fundamental aromatic substitution patterns, i.e. electron withdrawing carbonyl derivatives COX (COOH, COOR, CONH; 48% of aromatic integral), electron-neutral R (aliphatic and hydrogen; 23% of aromatic integral), and electron-donating OR (OH, OR, SR; 29% of aromatic integral) substituents, occupy typical chemical shift ranges indicated in color (Hertkorn et al., 2006; Perdue et al., 2007)

able chemical diversity discovered here very probably represents a very minimal assessment of molecular diversity actually present in the Soltmany L6 chondrite. Compared with the Murchison CM2 organic chondrite, the organic chemical diversity in Soltmany L6 chondrite appears more restricted; about half of Murchison's chemical compositions were common to both meteorites, whereas Soltmany's unique compounds comprised roughly 10% of the total mass peaks.

Proton NMR spectroscopy, which analyses chemical environments of dissolved molecules, has allowed for a near-quantitative assessment of proton chemical environments at lower sensitivities than FT-ICR mass spectrometry. This method has revealed both the

dominance of pure aliphatic spin systems (CCH) with short chain lengths (C_{3-4} units; in accordance with Remusat et al., 2005) in Soltmany L6 methanolic extract as well as the occurrence of oxygenated aromatics: nearly 80% of aromatics carried at least one oxygen, either as carbonyl derivatives (50%) or by means of direct oxygenation (30%). Aliphatic carboxylic acids comprised nearly 7% of aliphatics, based on proton NMR section integral (Fig. 6).

More precisely, NMR spectra of the Soltmany meteorite were acquired in deuterated methanol (CD_3OD) in order to suppress the otherwise huge solvent NMR resonance ($\delta_{\text{H}} = 3.30$ ppm). ^1H NMR

Table 1. Section ^1H NMR integral of non-exchangeable protons in Soltmany methanolic extract (Fig. 6)

NMR chemical shift, δ_{H} [ppm]	10–5	5–3.1	3.1–0.5
key substructure	$\text{C}_{\text{sp}}^2\text{H}$	OCH	CCH
relative abundance [%]	3.8	7.5	88.7

spectroscopy only detects HCD2OD; Fig. 6), given the rather low abundance of meteorite organic matter in solution. The ^1H NMR spectrum of Soltmany extract (Fig. 6) depicted non-exchangeable protons; all exchangeable protons (i.e. $-\text{XH}$, with X: O, N, S in common functional groups such as $-\text{OH}$, $-\text{COOH}$, and $-\text{NH}-$) were superimposed on the residual water resonance (HDO, $\delta_{\text{H}} = 5.02$ ppm), which has been suppressed here for improved visibility of Soltmany's organic matter.

The total range of the proton NMR chemical shift was first divided into purely aliphatic groups (CCH ; heteroatoms ≥ 3 bonds away from hydrogen; δ_{H} : 0...3.1 ppm), singly heteroatom-containing groups (OCH ; heteroatoms two bonds away from hydrogen, most likely oxygen; δ_{H} : 3.1...5.0 ppm) and unsaturated chemical environments [$\text{C}_{\text{sp}}^2\text{H}$; hydrogen bound to sp^2 -hybridized carbon, i.e. olefinic (here: $\delta_{\text{H}} \sim 5.3$ ppm), and aromatic protons ($\delta_{\text{H}} \sim 6.5$...8.0 ppm)].

Proton NMR spectra were in essence quantitative. Soltmany's methanolic extract featured large abundances of aliphatic protons. Additionally, about one-tenth of non-exchangeable protons were bound to heteroatoms (likely oxygen) and a minor suite (< 5%) of unsaturated protons was also observed (Tab. 1). The observed abundance distribution was partly caused by the lesser solubility of unsaturated chondritic matter in comparison with aliphatic compounds.

Within the aromatic section of chemical shift, chemical shift-based-discrimination of molecules was feasible because of electronic substituent effects. Electron-withdrawing substituents such as carbonyl derivatives COX caused downfield chemical shifts ($\delta_{\text{H}} > 7.3$ ppm) for aromatic ortho and para positions; electroneutral substituents such as alkyls and hydrogen caused intermediate chemical shifts ($\delta_{\text{H}} \sim 7.0$...7.3 ppm), whereas electron-donating groups caused upfield chemical shifts ($\delta_{\text{H}} < 7.0$ ppm; the electron-donating effect of electronegative substituents results from resonance interactions; Perdue et al., 2007). In Soltmany extract, the ratio of electron-withdrawing, electroneutral, and electron-donating aromatic substitution was 48/23/29 (Fig. 6), indicating considerable carboxylation of aromatic units. One single com-

pound with strong NMR resonances produces almost one third of the total aromatic NMR integral (Fig. 6). Three positions of chemical shifts with characteristic splitting ($\delta_{\text{H}} = 7.150$ ppm, 2H, $J_{\text{HH}} = 7.5$ and 8.2 Hz; $\delta_{\text{H}} = 6.785$ ppm, 1H, t, $J_{\text{HH}} = 7.3$ Hz; $\delta_{\text{H}} = 6.747$ ppm, 2H, d, $J_{\text{HH}} = 8.0$) indicated a $\text{C}_6\text{H}_5\text{OZ}$ unit with a yet-unidentified substituent Z (Z is not H as shown by comparison with ^1H NMR of methanolic phenol; data not shown). This $\text{C}_6\text{H}_5\text{OZ}$ unit was also confirmed by two-dimensional ^1H , ^1H TOCSY NMR spectra (Fig. 7).

Two-dimensional NMR spectra in general indicate pairs of atoms rather than individual atoms; the NMR experiment determines the interaction shown [e.g. spatial proximity (^1H , ^1H NOESY NMR spectra), homonuclear J couplings ($^2,^3J_{\text{HH}}$: COSY NMR spectra; $^nJ_{\text{HH}}$: TOCSY NMR spectra, commonly $n \leq 5-6$), and heteronuclear J couplings ($^1J_{\text{CH}}$: HSQC NMR spectra; $^nJ_{\text{CH}}$: HMBC NMR spectra, commonly $n \leq 2-3$)]. Homonuclear 2D NMR spectra relate two identical NMR spectra and initially show so-called diagonal peaks, in essence reflecting 1D NMR spectra with low resolution and negligible information content. The useful information is derived from the off-diagonal cross peaks, which indicate connectivities of atom pairs defined by respective NMR experiments (Macomber, 1998).

^1H , ^1H TOCSY NMR spectra allow a sensitive depiction of proton-proton couplings $^nJ_{\text{HH}}$ within proton NMR spin systems. According to sections of chemical shift, purely aliphatic spin systems ($\text{HC}-\text{C}_n-\text{CH}$; n : 0–4) resonate below $\delta_{\text{H}} < 3$ ppm (Fig. 7, panel A, box a). Spin systems with one heteroatom ($-\text{O}-\text{HC}-\text{C}_n-\text{CH}$; n : 0–4) show one participating proton in the aliphatic section ($\delta_{\text{H}} < 3$ ppm) and one participating proton in the heteroatom section ($\delta_{\text{H}} > 3$ ppm; Fig. 7, panel A, box b). Note the relative scarcity of double-heteroatom-containing aliphatic spin systems ($\text{X}-\text{O}-\text{HC}-\text{C}_n-\text{CH}-\text{O}-\text{Y}$; n : 0–4, X, Y: any substitution) in Soltmany methanolic extract: only very minor TOCSY cross peaks were found with chemical shifts δ_{H} : 3.0...5.0 ppm (Fig. 7, panel A). Intra-aliphatic spin systems in Soltmany extract were numerous (Fig. 7) and likely represented a superposition of several common chemical environments. Pure aliphatics are terminated by methyls; here, the ratio of methyl/total aliphatics was close to one-third (Fig. 6). Given that the H/C ratio of methyl is 3 and that of the other aliphatics is near 1.3 (in analogy to common chondritic organic matter), about every seventh carbon of Soltmany aliphatics is methyl. Methyl-terminating aliphatics show a lesser chemical diversity than do other aliphatics, because variance in substitution extends solely in one direc-

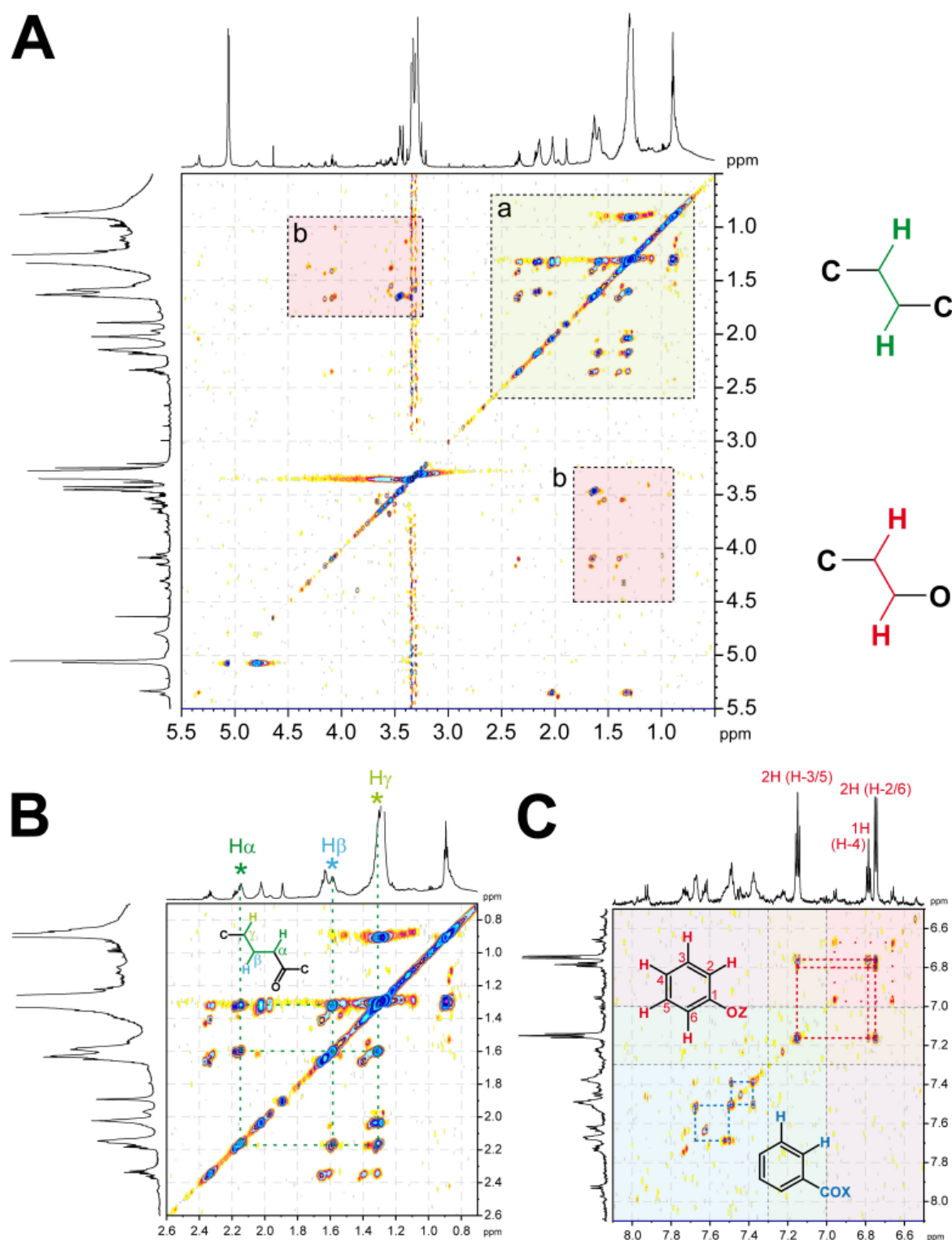


Fig. 7. 800 MHz ¹H, ¹H TOCSY NMR spectra of methanolic extract of Soltmany meteorite. Panel A: section of aliphatic cross peaks with purely intra-aliphatic cross peaks, section a: (C-CH-CH-C cross peaks) as well as oxygenated aliphatic units, section b: (C-CH-CH-O cross peaks) indicated. Panel B: enlarged section (panel A, section a) of intra-aliphatic cross peaks with a plausible spin system indicated. H_α resonates downfield of δ_H - 2.14 ppm and likely denotes protons in δ-position to carbonyl groups. With increasing distance, protons show progressively lower values of chemical shift [δ(H_β) - 1.59 ppm; δ(H_γ) - 1.31 ppm]. Polymethylene, i.e. long aliphatic chains, resonate near δ_H - 1.28 ppm, depending on proximate and remote substitution. This resonance produce a rather expansive consolidated cross peak of many similar chemical environments. Chain-terminating methyl groups resonate below δ_H < 1.0 ppm. Panel C: section of aromatic TOCSY cross peaks (X-C_{ar}-H-C_{ar}-H-Z; with two main spin-systems denoted according to characteristic patterns of chemical shift and spin-spin coupling (δ_H = 7.15 ppm, 2H, dd, J = 8.3, 7.5 Hz; δ_H = 6.79 ppm, 1H, t, J = 7.3 Hz; δ_H = 6.75 ppm, 2H, d, J = 8.0 Hz) very likely indicates an oxygen-substituted benzene H₂C₆OZ (Z: R, SO_nR with n = 0–3). The two downfield spin systems from δ_H -7.38 ... 7.78 ppm most probably denote carbonyl derivatives of benzene rings with vicinal proton pairs (i.e. protons bound to adjacent carbon positions)

tion. In contrast, methine carbon ($C_3\text{CH}$) allows for freedom in substitution in three directions. Hence, aliphatic methyl resonates at a rather narrow chemical shift range (here: $\delta_H \sim 0.7\text{--}1.2$ ppm). Carbonyl derivatives COX were likely substituents in Sołtmany organic matter, imposing downfield chemical shifts for adjacent protons ($\delta_H > 2.1$ ppm; Fig. 6), and common chemical shifts for typical aliphatic chemical environments (Fig. 7; Panel B). With respect to distance from carbonyl, (α -, β -, γ -, Fig. 7, panel B) aliphatic positions resonated at certain proton NMR chemical shifts. Similarly, pure aliphatic (e.g. linear and branched) hydrocarbons resonated within this chemical shift range (commonly $\delta_H < 1.6$ ppm; alicyclic rings more often resonated downfield from $\delta_H \sim 1.2$ ppm than open chain aliphatics). Polymethylene units, abundant in common biomolecules (like fatty acids, plant waxes) resonate at $\delta_H \sim 1.2$ ppm but were not preferred in meteoritic organic matter, in which a near statistical distribution of aliphatic branching motifs was found. Hence, the rather large ^1H NMR resonance at $\delta_H \sim 1.32$ ppm observed in Sołtmany methanolic extract probably resulted from the superposition of many purely aliphatic chemical environments; this was corroborated by the large number (> 10) of ^1H , ^1H TOCSY cross peaks related to this NMR resonance (Fig. 7; Panel B). In conclusion, Sołtmany aliphatics were composed of abundant branched hydrocarbons with $\sim 7\%$ of protons adjacent to carbonyl derivatives (likely carboxylic acids) and similar amounts bound to oxygen; substantial aliphatic branching was deduced from the $\text{CH}_3/\text{C}_{\text{aliphatic}}$ ratio in the range of 1:7.

The ^1H , ^1H TOCSY NMR spectrum showed the characteristic cross peaks of a $\text{C}_6\text{H}_5\text{OZ}$ unit; i.e. the spin system is composed of a single (para, 1H) proton and both ortho and meta positions (2H each because of magnetic equivalence) exhibit TOCSY cross peaks (Fig. 7, Panel C). In addition, several carboxylated aromatic rings show downfield ($\delta_H < 7.4$ ppm) cross peaks, indicating multiple carboxylations.

Considering the strong thermal alteration of Sołtmany L6 chondrite, the provision of extensive EOM chemical diversity suggests that investigating organic chemical diversity in any pristine or thermally altered meteorite will offer encouraging clues about its

formation and evolution. It is still too early for us to understand the intimate processes involved in the formation of these compounds, and we will need to systematically investigate fresh meteoritic falls of different classes and petrologic types to assess the significance of the chemical complexity and diversity we unexpectedly discovered with this study. Intimate organo-mineral interactions (Kleber et al., 2007; Schoonen et al., 2004), which are known to protect terrestrial (e. g. soil and sedimentary) organic matter from rapid degradation, might have provided additional means of EOM generation and conservation. A rich diversity of minerals acting as sorbents, catalysts, and templates all offer the capacity to initiate crucial transformations of primordial volatile precursor molecules (CO , CO_2 , H_2 , CS , H_2O , HCN , NH_3 , H_2S , HCHO) into simple organic molecules (~ 10 atoms) and the consecutive assembly of ever larger compounds. The minerals' chemical compositions, morphologies, distributions of impurities, and presence of structural and/or electronic defects as abundantly found in chondrites will decisively affect the specificity of these organo-mineral interactions (Schoonen et al., 2004) responsible for the generation and decomposition of organic molecules throughout the history of EOM formation. Here, an extensive and largely unknown organic molecular complexity meets an appreciable and passably understood mineral heterogeneity ranging from nanoscales (e.g. electronic and structural defects; shape selectivity) to microscales (crystal symmetry and surface properties), of which a limited fraction has been explored in more than 50 years of industrial catalysis (Pérez-Ramírez et al., 2008; Smit and Maesen, 2008).

It is conceivable that (formerly hot) mineral surfaces within porous parent bodies might have catalyzed bond formation in-between small and possibly vaporized organic molecules, contributing to the assembly of those precursors into larger compounds. These smaller molecules were then subject to preferential deposition in narrow cavities of abundantly available large interior mineral surfaces (Le Guillou et al., 2012). Furthermore, active organo-mineral interactions will likely limit the solubility of OM in organic solvents; i.e. the proportions of soluble and insoluble organic matter (IOM) could then shift towards IOM.

CONCLUSION

We first made an inventory of the polar solvent extractable organic matter from the L6 ordinary chondrite that fell in Sołtmany and showed the presence of thousands of different CHNOS-type of molecules. More studies are needed to describe the chemical

footprints of extracts from various petrologic types of chondrites on a molecular level, involving a parallel characterization of the insoluble organic matter (IOM) in order to describe the various chemical diversities and better understand the structural origin

of the present organic matter. On-going studies will employ additional extraction procedures with protic/aprotic solvents to extract molecules of various polarities. The known limitations of electrospray ionization in ionizing non-polar molecules will require the use of alternative ionization techniques such as photoionization or chemical ionization to generate a more significant assessment of organic molecular diversity. The molecular characterization of CH, CHN or CHS type of compounds will contribute to a better understanding of the processes leading to the formation and stabilization of particular organic chemistry discovered in ordinary chondrites.

This study also demonstrated the yet-untapped opportunities that arise from the collection of structural information of organic compounds extracted from a pristine, freshly fallen sample. Our investigations underline the importance of protecting freshly fallen meteorites from terrestrial contamination or weathering

that could occur over time, modifying their pristine organic compositions, thereby, interfering in later global organic analyses. The sooner after a fall an analysis can be performed, the better the odds that (chemical and biological) contaminations can be limited. It would be perfectly adequate to avoid direct handling with skin contact and to eliminate the potential for terrestrial corruption by cooling the sample with liquid nitrogen directly after the fall; this might be more feasible with meteorites that have fallen in Antarctica. Even if inconvenient, the insights derived from the organic analysis of pristine meteorite samples will provide invaluable clues about meteorites' histories and their pathways of chemical evolution in general. Studies currently being performed with other fresh falls such as the carbonaceous chondrite Sutter's Mill and Shergottite Tissint confirm the presence of specific organic signatures changing as a function of the petrologic type (Schmitt-Kopplin et al., 2012a, 2012b).

ACKNOWLEDGEMENTS

We gratefully thank Dr Tomasz Jakubowski and Prof. Tadeusz A. Przylibski, Wrocław University of Technology, Institute of Mining Engineering, Wrocław, Poland for sending us the Sołtmany sample for analysis; at the time we were asking for a sample

for analysis, it certainly was not trivial to think that in L6 type meteorite would contain much in the way of organic compounds. Also we thank the unnamed reviewers who proposed additional changes that improved this manuscript.

REFERENCES

- Alexander C.M., Boss A.P., Carlson R.W., 2001 – The early evolution of the inner solar system: a meteorite perspective. *Science*, 293, 64-68.
- Cody G.D., Alexander C.M.O., Yabuta H., Kilcoyne A.L.D., Araki T., Ade H., Dera R., Fogel M., Militzer B., Mysen B.O., 2008 – Organic thermometry for chondritic parent bodies. *Earth And Planetary Science Letters*, 272, 446-455.
- Grady M.M., Wright I.P., Pillinger C.T., 1989 – A preliminary investigation into the nature of carbonaceous material in ordinary chondrites. *Meteoritics*, 24, 147-154.
- Haack H., Grau Th., Bischoff A., Horstmann M., Wasson J., Norup Sørensen A., Laubenstein M., Ott U., Palme H., Gellissen M., Greenwood R.C., Pearson V.K., Franchi I.A., Gabelica Z., Schmitt-Kopplin Ph., 2012 – Maribo – a new CM fall from Denmark. *Meteoritics & Planetary Science*, 47 (1), 30-50.
- Herd C.D.K., Blinova A., Simkus D.N., Huang Y., Tarozo R., Alexander C.O.D., Gyngard F., Nittler L.R., Cody G.D., Fogel M.L., Kebukawa Y., Kilcoyne A.L.D., Hilt R.W., Slater G.F., Glavin D.P., Dworkin J.P., Callahan M.P., Elsila J.E., De Gregorio B.T., Stroud R.M., 2011 – Origin and Evolution of Prebiotic Organic Matter As Inferred from the Tagish Lake Meteorite, *Science*, 332, 1304-1307.
- Hertkorn N., Benner R., Schmitt-Kopplin Ph., Kaiser K., Kettrup A., Hedges I.J., 2006 – Characterization of a major refractory component of marine organic matter. *Geochimica et Cosmochimica Acta*, 70 (12), 2990-3010.
- Hertkorn N., Ruecker C., Meringer M., Gugisch R., Frommberger M., Perdue E.M., Witt M., Schmitt-Kopplin Ph., 2007 – High-precision frequency measurements: indispensable tools at the core of the molecular-level analysis of complex systems, *Analytical Bioanalytical Chemistry*, 389, 1311-1327.
- Hertkorn N., Frommberger M., Schmitt-Kopplin Ph., Witt M., Koch B., Perdue E.M., 2008 – Natural Organic Matter and the Event Horizon of Mass Spectrometry. *Anal Chem.*, 80, 8908-8919.
- Karwowski Ł., 2012 – Sołtmany meteorite. *Meteoritics*, 2 (1-2), 15-30 (this number).
- Karwowski Ł., Pilski A.S., Przylibski T.A., Gattacceca J., Rochette P., Łuszczek K., Kryza R., Woźniak B., Woźniak M., 2011 – A new meteorite fall at Sołtmany, Poland. 74th Annual Meteoritical Society Meeting, 5336pdf.
- Kebukawa Y., Conel A., Cody G.D., 2011 – Compositional diversity in insoluble organic matter in type 1, 2 and 3 chondrites as detected by infrared spectroscopy. *Geochimica et Cosmochimica Acta*, 75, 12, 3530-3541.
- Kim S., Rodgers R.P., Marshall A.G., 2006 – Truly "exact" mass: Elemental composition can be determined uniquely from molecular mass measurement at similar to 0.1 mDa accuracy for molecules up to similar to 500 Da. *International Journal of Mass Spectrometry*, 251, 260-265.
- Kleber M., Sollins P., Sutton R., 2007 – A conceptual model of organo-mineral interactions in soils: self assembly of organic molecular fragments into zonal structures on mineral surfaces. *Biogeochemistry*, 85, 9-24.

- Le Guillou C., Rouzaud J.-N., Bonal L., Quirico E., Derenne S., Remusat L., 2012 – High resolution TEM of chondritic carbonaceous matter: Metamorphic evolution and heterogeneity. *Meteoritics & Planetary Science*, 47(3), 345-362.
- Macomber R.S., 1998 – A complete introduction to modern NMR spectroscopy, Wiley-Interscience, Chichester.
- Makjanic J., Vis R.D., Hovenier J.W., Heymann D., 1993 – Carbon in the matrices of ordinary chondrites. *Meteoritics*, 28, 63-70.
- Marshall A.G., Hendrickson C.L., Jackson G.S., 1998 – Fourier transform ion cyclotron resonance mass spectrometry: A primer. *Mass Spectrometry Reviews*, 1, 1-35.
- Perdue E.M., Hertkorn N., Ketrup A., 2007 – Substitution patterns in aromatic rings by increment analysis: Model development and application to natural organic matter. *Analytical Chemistry*, 79 (3), 1010-1021.
- Pérez-Ramírez J., Christensen C.H., Egeblad K., Christensen C.H., Groen J.C., 2008 – Hierarchical zeoliths: enhanced utilisation of microporous crystals in catalysis by advances in materials design. *Chemical Society Reviews*, 37, 2530-2542.
- Quirico E., Raynal P.I., Bourot-Denise M., 2003 – Metamorphic grade of organic matter in six unequilibrated ordinary chondrites. *Meteoritics & Planetary Science*, 38, 795-811.
- Remusat L., Derenne S., Robert F., 2005 – New insights on aliphatic linkages in the macromolecular organic fraction of Orgueil and Murchison meteorites through ruthenium tetroxide oxidation, *Geochimica et Cosmochimica Acta*, 69, 4377-4386.
- Smit B., Maesen L.M., 2008 – Towards a molecular understanding of shape selectivity. *Nature*, 451, 671-678.
- Schmitt-Kopplin Ph., Gabelica Z., Gougeon R.D., Fekete A., Kanawati B., Harir M., Gebefügi I., Eckel G., Hertkorn N., 2010 – High molecular diversity of extraterrestrial organic matter in Murchison meteorite revealed 40 years after its fall, *Proceedings of the National Academy of Sciences of the United States of America*, 107 (7), 2763-2768.
- Schmitt-Kopplin Ph., Gelencsér A., Dabek-Zlotorzynska, E., Kiss G., Hertkorn N., Harir M., Hong Y., Gebefügi I., 2010 – Analysis of the unresolved organic fraction in atmospheric aerosols with ultrahigh resolution mass spectrometry and nuclear magnetic resonance spectroscopy: Organosulfates as photochemical smog constituents. *Analytical Chemistry*, 82 (19), 8017-8026.
- Schmitt-Kopplin Ph., Harir M., Tziotis D., Gabelica Z. Hertkorn 2012a – Ultrahigh Resolution Fourier Transform Ion Cyclotron Resonance Mass Spectrometry for the Analysis of Natural Organic Matter from Various Environmental Systems. Chapter 19, In: Comprehensive Environmental Mass Spectrometry Edited by Albert Lebedev, ILM Publications. 443-459.
- Schmitt-Kopplin Ph., Harir M., Hertkorn N., Chennaoui Aoudjehane H., Fernández Remolar D.C., Hinman N., Gabelica Z., 2012b – High chemical diversity of solvent soluble polar fraction of the Tissint shergottite. *Meteoritics & Planetary Science*, Special Issue: The 75th Annual Meeting of the Meteoritical Society, Cairns, Australia, August 12-17, 2012, 5356.
- Schmitt-Kopplin Ph., Harir M., Hertkorn N., Jenniskens P., Gabelica Z., 2012c – Unusual chemical diversity of solvent soluble polar fraction of the Stutter's Mill Carbonaceous chondrite. *Meteoritics & Planetary Science*, 2012, Special Issue: The 75th Annual Meeting of the Meteoritical Society, Cairns, Australia, August 12-17, 2012, 5359.
- Schoonen M., Smirnov A., Cohn C., 2004 – A Perspective on the Role of Minerals in Prebiotic Synthesis, *Ambio*, 33, 539-551.
- Tziotis, D., Hertkorn, N., Schmitt-Kopplin, Ph., 2011 – Kendrick-analogous Network Visualisation of Ion Cyclotron Resonance Fourier Transform (FTICR) Mass Spectra: Improved Options to Assign Elemental Compositions and to Classify Organic Molecular Complexity. *European Journal of Mass Spectrometry*, 17, 415-421.
- Wadi J., Woreczko J., 2011 – Soltmany, A New Polish Meteorite Fall. *Meteorite*, August 2011. http://www.woreczko.pl/meteorites/travels/Soltmany_2011/Soltmany-EN.htm.
- Weisberg M.K., McCoy T., Krot A.N., 2006 – Systematics and evaluation of meteorite classification, [in:] D.S. Lauretta, H.Y. McSween (eds), Meteorites and the Early Solar System II, Ed. by 19-52.
- Woods J.A. 2005 – The chondrite types and their origins, [in:] Chondrites and the protoplanetary disk, ASP Conference Series, 341, 953-971.
- Zenobi R., Philippos J.M., Zare R.N., Wing M.R., Bada J.L., Marti K., 1992 – Organic compounds in the Forest Vale, H4 ordinary chondrite. *Geochimica et Cosmochimica Acta*, 56, 2899-2905.

APPENDIX 1. PRINCIPLES OF FT-ICR-MS

Ion cyclotron resonance mass spectrometry refers to the measurement of the cyclotron frequency of ions trapped inside a confined cylindrical geometry located inside a magnet (Marshall et al. 1998). Fig. A shows the ICR cell with an orbiting ion inside. Ions can be

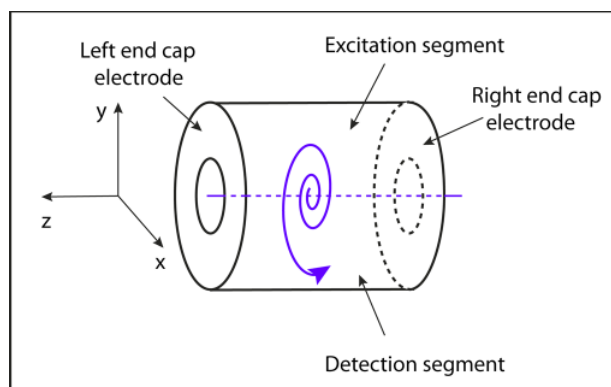


Fig. A. A cylindrical geometry of an ICR cell with two bored end cap electrodes. The blue spiral indicates a trajectory of an ion during radial (XY) ion excitation prior to detection. The central electrode is segmented four-fold with both counterpart segments representing either detector pairs or transmitter pairs

detected by their energy absorption from an external waveform generator that causes expansion of their cyclotron radius so that their orbits range in proximity to two detector plates located in the central ring electrode of the cell. Each ion m/z corresponds to a specific cyclotron frequency (Eq. 1). A mass spectrum (MS) represents a histogram, which shows different ion abundances as a function of m/z ratios. Mass spectra result from the detection of the cyclotron frequencies of all confined ions. This is achieved by performing a mathematical Fourier transform of the detected transient induced charge, collected as a function of time (Fig. B).

$$\omega_c = \frac{qB}{m} \quad (1)$$

The cyclotron frequency ω_c is given by Eq. 1, in which m is the ion mass in amu, q is the charge state, and B is the magnetic field strength in Tesla. It is obvious from Eq. 1 that higher magnetic field strength causes larger confined ion cyclotron frequencies, translating into higher mass resolving power.

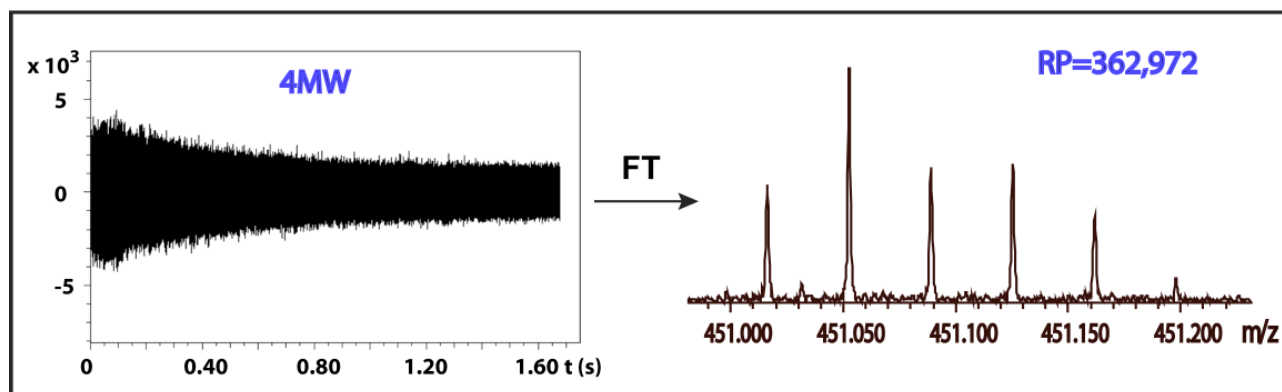


Fig. B. Acquisition of one a standard natural organic matter sample (Suwannee River surface water fulvic acid / FA, obtained from International Humic Substances Society – IHSS). The time domain detected transient is shown on the left, acquired with 4M data points within 1.6 seconds. Right: The mass spectrum is obtained as a result of Fourier transformation of the induced charge transient and application of Eq. 1. Here, the mass resolving power is 362,972 at $m/z = 451$

APPENDIX. 2. BASICS OF NMR SPECTROSCOPY FOR ELUCIDATION OF MOLECULAR STRUCTURES

NMR measures the precession frequencies of individual nuclear magnetic moments in an external magnetic field B_0 ; these depend on the nuclear properties (γ_N : gyromagnetic ratio), B_0 applied, and the local chemical environments. Hence, any atom within an organic molecule produces a unique NMR signature. This information-rich detection defines NMR spectroscopy as the most powerful method for the structural analysis of amorphous materials currently available. For

instance distinguishing between isomers using this process is facile (Fig. C). Common isotopes used in the structural elucidation of organic compounds are the spin $\frac{1}{2}$ nuclei ^1H , ^{13}C , ^{15}N and ^{31}P ; note that the common nuclei ^{12}C , ^{16}O and ^{32}S do not exhibit a magnetic moment (nuclear spin $I = 0$) and therefore cannot be used for NMR spectroscopy (Macomber, 1998).

Tab. A. Three key NMR parameters useful for structural analysis of organic molecules

Parameter	Acronym	Appearance in NMR spectrum	Significance in structural analysis
Chemical shift	δ	position of NMR resonances on the horizontal (frequency) axis	defines chemical environment of all neighboring atoms. δ denotes the fractional change in precession frequency of a specific nucleus induced by the variance in chemical environments normalized to B_0 , typically given in [ppm]
Spin-spin coupling	$^nJ_{AB}$	multiplicity of NMR resonances	spin-spin coupling constant for nuclei A and B through "n" bonds [Hz]; refers to count of adjacent nuclei
Integral	S	integrated signal intensity	signal intensity integrated across a full multiplet, denotes quantity of magnetically equivalent nuclei

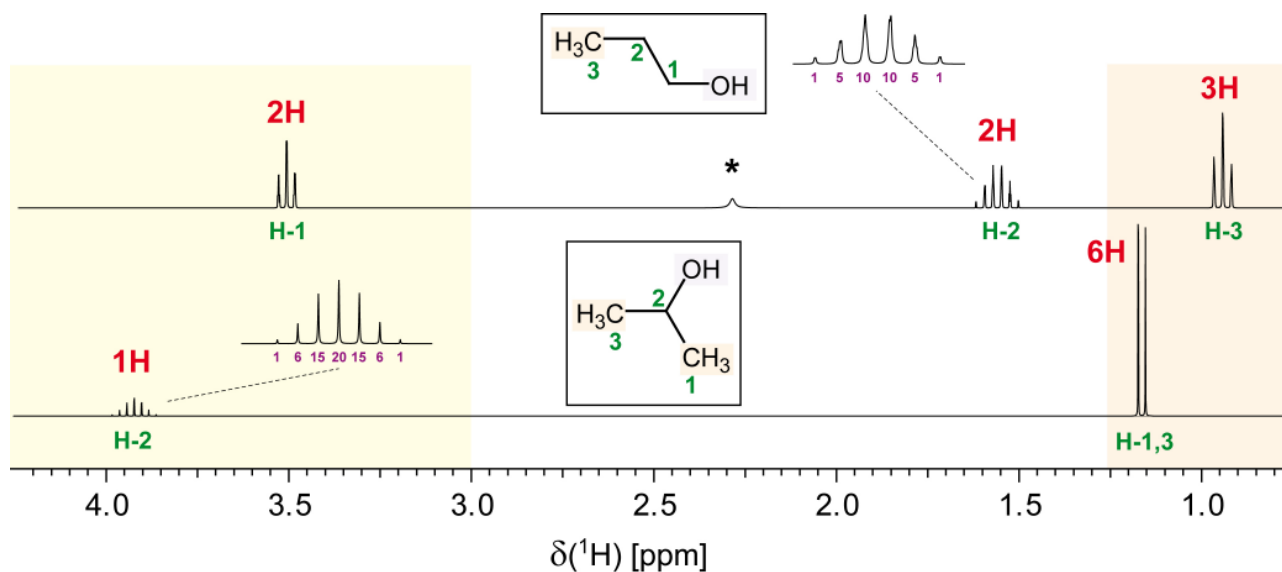


Fig. C. ^1H NMR spectra (300 MHz, computed) of two isomers of $\text{C}_3\text{H}_8\text{O}$ with assignments (asterisk denotes the exchangeable hydroxyl proton which is out of range in case of isopropanol). Red numbers denote NMR integrals; NMR signal splittings indicate J-couplings, which denote counts of adjacent nuclei according to the equation $2 \times n \times I + 1$ [n : number of magnetically equivalent neighbors, I : nuclear spin ($^1\text{H}) = \frac{1}{2}$]. In isopropanol (bottom row), a single proton (H-2; integral 1H) and six magnetically equivalent protons (H-1,3; integral 6H) from two methyl groups define the overall spin system of non-exchangeable protons. H-2 is split into seven signals (septet, $2 \times 6 \times \frac{1}{2} + 1 = 7$, with intensity distribution according to Pascal's triangle) and H-1,3 into two signals (doublet, $2 \times 2 \times \frac{1}{2} + 1 = 2$). Similarly, three groups of magnetically non-equivalent protons define the spin system of non-exchangeable protons in n-propanol (top row). These three groups are the chain-terminating methyl group (H-3; integral 3H, 1:2:1 triplet splitting from two adjacent methylene protons), the central methylene (H-2; integral 2H, sextet splitting from five neighboring protons, with intensity distribution according to Pascal's triangle), and the hydroxymethylene group (H-1; integral 2H, 1:2:1 triplet splitting from two neighboring methylene protons). Note that proximate oxygen causes a chemical shift $\delta_{\text{H}} > 3.0$ ppm (yellow shade), while methyl groups resonate near $\delta_{\text{H}} < 1.2$ ppm (orange shade). Hydroxy protons are typically subject to fast chemical exchange in solution and therefore produce rather broad 1H NMR resonances.